A Search for Red Giants as Tracers of the Dark Matter Mass Profile of the Milky Way.

A Thesis Submitted in Partial Satisfaction
Of the Requirements for the Degree of
Bachelor of Science in Physics
at the
University of California, Santa Cruz

By
Jonathan Y. Kemal
June 10, 2009

Professor Constance Rockosi Technical Advisor	David P. Belanger Supervisor of Senior Theses, 2001-2009

David P. Belanger
Chair, Department of Physics

TABLE OF CONTENTS

ABSTRACT

The recent discovery of Dark Matter lead to the realization that the majority of mass is our universe is not understood. Furthermore, the fact that this matter cannot be seen lead to the realization that the distribution of matter in our universe, as well as our own galaxy, is not well understood either [Ryden, 2003]. The purpose of this project is to find distant stars in the halo of our galaxy so that they can be used as test particles in the galaxy's gravitational potential, with the ultimate goal of developing a dark matter mass profile. As red giants can be hundreds of times brighter than main sequence stars (dwarfs), finding the desired halo stars is a matter of determining which faint stars are distant giants as opposed to relatively nearby dwarfs. While giants and dwarfs can be similar in surface temperate (color) and atmospheric metal abundance (metallicity), the strength of gravity at their surfaces differs greatly. An analysis of stellar spectra is necessary to classify stars, as temperature, chemical abundance, and internal pressure all have an effect on the structure of spectral absorption lines [Shu, 1982].

Unfortunately, existing classification methods involve analysis of small regions of stellar spectra and are thus only reliable for strong signal stars. This project involves the development of a new classification method that compares the spectrum of a test star to the spectra of known giants and dwarfs, which are similar to the star in both color and metallicity. Specifically, reduced χ^2 goodness-of-fit tests are used to compare spectra over the wavelength range of 3900-6100 Å, with the exception of the 50 Å range surrounding a molecular oxygen emission line at 5575 Å. Except where specifically noted, all data – whether spectral or photometric – were taken from the SDSS/SEGUE

online database DR7 [Yanny et al., 2009]. All comparisons, tests, and calculations were performed using IDL.

The classification technique as well as the library of known giants and dwarfs (template stars) was refined through various tests and analysis. Known giants that are a part of the globular cluster M13 were particularly useful for analysis, as the template library was tested against noisy versions of these spectra in order to determine quantitatively the likelihood of a correct classification as a function of S/N ratio [Yanny et al., 2009]. Currently, the template library consists of 87 giants and 88 dwarfs that have colors ranging between approximately 0.5 and 0.8 and span the metallicity range of roughly -2.5 to -1. It is expected that at least 90% of test stars with a S/N ratio of 11.5 or higher can be classified correctly. While analysis is ongoing, 9668 test stars have been initially classified as giants. The distances to these stars, both from the Earth and from the center of the galaxy, still need to be computed. A final list of halo giants is expected by August 2009.

I: INTRODUCTION

The formation of spiral galaxies remains among the most important unsolved problems in astronomy. As the majority of galaxies observed in the universe are spiral galaxies, understanding their formation and evolution is clearly a crucial aspect of understanding the development of structure in the universe as a whole. It is very fortunate that the Milky Way seems to be a typical spiral galaxy, as it is certainly easier to study than even its closest neighbors.

In order to understand how a galaxy forms and evolves, there first needs to be a good understanding of what the galaxy currently looks like. However, the recent discovery of dark matter has lead to the realization that an unknown type of matter accounts for the majority of the galaxy's mass. Not only is there a lack of understanding about what dark mater is, the fact that it is not visible makes it difficult to measure an accurate mass profile of the Milky Way. The galaxy's spiral disc and core, where ordinary matter is most concentrated, are surrounded by a relatively diffuse spherical halo of ordinary matter [Shu, 1982]. The dark matter in our galaxy, however, is believed to exist in the form of a spherical halo without being primarily concentrated in the galactic disc [Ryden, 2003]. A detailed description how this mass density changes as a function of radius has yet to be developed.

The purpose of the following project is to obtain a dark matter mass profile of the Milky Way. The natural way to do this is to study how distant stars, acting as test particles, move in the gravitational potential of the galaxy. While the techniques for studying this motion are not the subject of this thesis, the distance of the test particles clearly limits the depth to which a mass profile can be calculated. Thus, it is necessary to

find stars as far out in the galactic halo as possible. Finding distant halo stars, however, requires an understanding of the reasons that a star may be bright or faint in the sky. Most stars spend nearly all of their lives fusing hydrogen into helium in their cores, meanwhile varying little in mass, radius, or luminosity. Stars in this stage of their lives are referred to as main sequence stars. Once all the hydrogen in the core is used up, the star begins to evolve quickly and its radius beings to expand while its intrinsic luminosity increases dramatically. The star settles for some time in this state where hydrogen fusing is occurring in shells surrounding the core, instead of in the core itself. Somewhat counter intuitively, while its luminosity has increased its surface temperature has dropped significantly. This lower temperature typically results in these stars appearing red in color; they are subsequently called red giants [Shu, 1982][1]. Throughout this paper "giant" will refer to a red giant and does not have any implication on the actual mass of the star, similarly a "dwarf" will refer simply to a main sequence star.

One concern is that the remaining portions of stellar evolution, particularly those uniquely associated with stars that are much more massive than the Sun, could complicate the process of classifying stars[2]. Due to its diffuse nature, the galactic halo is not an area of active star formation and since it is believed that it is a remnant of our galaxy's formation, it is expected that the halo stars are billions of years old. As the lifespan of a star is inversely related to its mass, stars many times more massive than the sun live only a few hundred million years. It is therefore expected that the halo stars that still exist have roughly the mass of our Sun. While the previously discussed "red giant" phase is not the end of a solar mass star's life, the last phases of their evolution happen

[1] Shu provides a significantly more detailed overview of stellar evolution.

[2] Shu describes the evolution of very massive stars, which differs significantly from that of solar mass stars.

rapidly and thus it is inherently unlikely that a halo star will be anything other than a dwarf or a giant as previously defined [Shu, 1982].

Although time has limited the types of stars that still exist in the halo, finding distant stars remains a difficult task. As illustrated by Fig. 1, a star might become several hundreds of times more luminous as it evolves into a red giant. This results in distant halo giants appearing similar in brightness to relatively nearby dwarfs. Clearly, finding distant stars in the halo requires the ability to determine why the stars appear faint: whether they are giants or dwarfs. Unfortunately, classifying faint objects is not a trivial task. Despite the nuclear reactions in their cores and the features of their spectra, stars can be approximated fairly accurately as ordinary black bodies [Shu, 1982]. The energy density of radiation as a function of wavelength and temperature can thus be approximated using Plank's law for ideal blackbodies [Tipler and Llewellyn, 2003].

$$u(\lambda) = \frac{8\pi hc\lambda^{-5}}{e^{hc/\lambda KT} - 1} \qquad (1)$$

As Plank's law shows, the intensity of light being emitted by a star varies as a function of both the frequency of the light and the surface temperature of the star. Simply put, the color of a star depends on its surface temperature. The surface temperature of a star, however, is dependent on its mass. As a result, despite the fact that a star reddens in color as it evolves into a giant, there are both giants and dwarfs which range in appearance from very red to very blue [Shu, 1982]. The following isochrones, also known as a Hertzsprung–Russell (HR) diagrams, show how the intrinsic brightness of stars can vary as a function of their surface temperature.

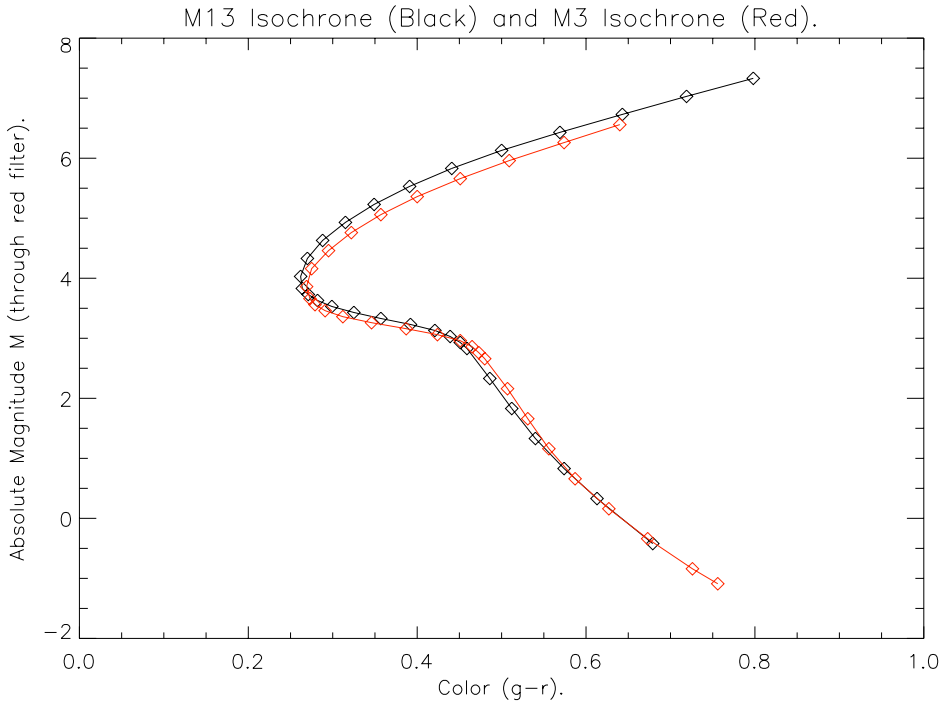

Figure 1: An Isochrone of stars in the M3 and M13 globular clusters generated with data taken from An et al., 2008.

The above isochrone consists of the absolute magnitude of many stars plotted against a quantified measurement of their color: the difference in apparent magnitude through a green filter and red filter. The photometric data correspond to stars in two globular clusters, which are discussed in greater detail in section IV [An et al., 2008]. The magnitude scale is a logarithmic scale for measuring the brightness of celestial objects. Apparent magnitude, m, refers to how bright a star appears from earth and absolute magnitude, M, refers to the brightness an observer would measure if he were a distance, D, 10 parsecs for stars, from the object [Shu, 1982].

$$M = m - 5\log_{10}(D) + 5 \tag{2}$$

According to the definitions of the magnitude scale, it can be shown that a difference in apparent magnitude of 5 corresponds to a factor of 100 in intrinsic brightness. Keeping in mind that Fig. 1 is a plot of absolute magnitude, and that lower

numbers represent brighter stars on this scale, the bottom "branch" clearly represents giants that are in some cases hundreds of times more luminous than dwarfs that are similar in color (the top branch).

Fortunately, there is one physical property that distinctly separates the giants from dwarfs: the strength of gravity near the surface of the star. A star's internal pressure, generated ultimately by nuclear reactions, is what supports it against the inward pull of gravity. This equality of pressure and gravity, called hydrostatic equilibrium, implies that that the internal pressure in the atmosphere of a giant differs significantly from that of a dwarf. While the details are somewhat involved, three factors primarily dictate the strength and width of spectral absorption lines: the surface temperature of the star, internal pressure, and the abundance of relevant elements or molecules in the stellar atmosphere [Shu, 1982]. Due to the fact that surface temperature and atmospheric chemical abundance fail to give information as to whether a star is a giant or a dwarf, the effects of internal pressure on spectral absorption lines must be analyzed in order to classify a star.

It seems there is no short cut. In order to obtain a sample of distant halo stars, faint objects need to be classified which can only be done by analyzing the individual spectra of the stars. Unfortunately, the faintness of the stars, which makes them appealing in the first place, also makes them difficult to classify. Popular classification methods involve the analysis of specific spectral absorption lines [Shu, 1982]. Assuming a constant exposure time, which is the case for this project[3], faint stars have very low signal/noise (S/N) ratios, meaning the flux received from the star is not very much higher

[3] See Yanny et al., 2009 for definition of exposure time.

than the flux of ambient noise [Yanny et al., 2009]. In other words, the statistical uncertainty of the strength or width of any specific spectral line is too high for existing classification methods to be reliable.

In order to achieve the goal of this project, a new technique of classifying weak signal stars had to be developed. The basic idea is that a weak signal star can be classified by comparing a large portion of its spectrum to the spectra of previously classified high signal stars that are similar in color as well as atmospheric metal abundance (metallicity). Here, as will be discussed in section II, a star's color is quantitatively defined as the difference in the star's apparent magnitude measured through the g (green) and r (red) filters used for SDSS/SEGUE[4]. The color values used also attempt to correct for extinction. Extinction values are quantitative estimates (on the magnitude scale) of the loss of brightness due to absorption of light by gas, dust, etc. in the interstellar medium. Metallicity, estimated by the SDSS pipeline is a measurement of the amount of iron in a star, quantitatively defined by (3) where the N values refer to the estimated number of atoms of the specific element in the star [Yanny, et al., 2009].

$$[F_e/H] = \log_{10}\left(\frac{N_{Fe,star}/N_{H,star}}{N_{Fe,solar}/N_{H,solar}}\right) \tag{3}$$

The use of large comparison regions eliminates the need for precise measurements of the strength of specific spectral lines and instead relies on the idea that, even at low signal, the spectrum of a star should on average resemble the spectrum of a previously classified star of the same type. However, various phenomena need to be understood and corrected for before these comparisons can be made. These issues, as well as the comparison process itself, are discussed in section III.

[4] See Yanny et al., 2009 for definitions of color filters and a description of how extinction values and metallicity are estimated.

II: DATA

All stars used for this project were observed as part of the Sloan Digital Sky Survey (SDSS) and the Sloan Extension for Galactic Understanding and Exploration (SEGUE) [Yanny et al., 2009]. Except where specifically discussed in section IV, all relevant data were obtained directly from the SDSS online database DR7[5]. The original library of template stars consisted of 244 previously classified stars, 111 giants and 113 dwarfs, spanning the color range of approximately 0.5-1.3 and the metallicity range -2.5 to -1. In addition, the library consisted of 20 stars, previously classified as giants, which are part of the globular cluster M13 and span roughly the same range in color[6]. All initial classifications of template stars are based upon the values for surface gravity[7] estimated by the SDSS pipeline, which employs existing classification techniques [Yanny et al., 2009]. As all template stars are relatively bright and have strong signal, these classifications are assumed to be correct. The metallicity of M13 is taken to be approximately -1.6 which is fairly well centered within the range spanned by the other template stars. However, as discussed in detail in section IV, various tests lead to the reduction of this library and the decision to use new photometric data for the M13 giants [An et al., 2008]. The template library currently consists of 155 template stars, 87 giants (Including 14 M13 giants) and 68 dwarfs, spanning the color range of roughly 0.5-0.8 as well as the same range in metallicity as previously mentioned. The complete template library can be found in the Appendix.

---

[5] The SDSS DR7 database can be found at http://www.sdss.org/dr7/

[6] One M13 giant has an estimated color value of 1.6. This star is not concluded in the final template library.

[7] Surface gravity measurements given by the entry "logga" of the "sppParams" table in the DR7 database.

III: PROCEDURE

III.1: Reduced χ^2 Goodness-of-Fit Test

The technique developed for the classification of low signal test stars is fairly straightforward. As described above, the test star needs to be compared over a large region of the stellar spectrum with a library of template stars that are similar to it in color and metallicity. The method used to quantitatively compare the spectra is a reduced χ^2 goodness of fit tests over the wavelength range of 3900 -6100 Å, but excluding the 50 Å region surrounding an emission line at 5575 Å (see section IV).

$$\chi^2 = \frac{1}{N}\sum_n \frac{\left(template_n - test_n\right)^2}{\sigma^2_{template,n} + \sigma^2_{test,n}} \tag{4}$$

$Template_n$ and $test_n$ refer to the flux at the n^{th} pixel (corresponding physically to a specific wavelength of light) for the template and the test star, respectively. N refers to the total number of pixels in the comparison range. While the same wavelength range is consistently used, the value of N changes slightly due to the effects of redshift discussed below. Similarly, the σ_n values refer to the measured value of ambient noise at the given pixel. For this purpose, low signal test stars are being compared against high signal templates, and thus, particularly after squaring the values, the noise associated with the template is negligible and $\sigma_{template,n}$ can be ignored. As the noise appears in the denominator of the sum, accounting for it helps to reduce the total χ^2 value. Here, the reduction helps ensure that the χ^2 values do not differ too significantly as a function of the apparent magnitude of the test star. That is, two test stars of the same color and metallicity (and thus compared against the same templates) should produce somewhat similar χ^2 values – despite a significant difference in apparent brightness. In other words, the reduction helps to ensure that χ^2 values are a reflection of similarities in features of

stellar spectra and not simply the strength of the signal. Looking at (4), it is clear that the χ^2 value will be small if the template and test star are consistently similar in value. Thus, a small χ^2 value is expected to represent a good match.

III.2: Correcting for Redshift

Before a χ^2 comparison can be made, various physical phenomena need to be accounted for. Halo stars are sometimes moving at more than 200 km/s, which causes a significant Doppler effect and a corresponding redshift that needs to be removed. While such speeds are hard to imagine, they are still much too slow to be considered relativistic and the Doppler effect can therefore be treated classically [Serway, 2004].

$$\lambda_{observed} = \left(\frac{c \pm v_{Star}}{c} \right) \lambda_{emitted} \tag{5a}$$

$$z = \frac{\lambda_{observed} - \lambda_{emitted}}{\lambda_{emitted}} \tag{5b}$$

The measurement of the strength of this effect, z, is called the redshift. The velocity, v_{star}, is the line of sight velocity and is defined such that a positive value represents motion away from the observer. Since the wavelength at which various gasses emit spectral lines are well known for gasses at rest, the value of a star's redshift can be calculated by looking for these emission lines in the star's spectrum and then estimating the difference in the observed and emitted wavelengths. The redshift values of all templates and test stars were calculated by the SDSS pipeline [Yanny et al., 2009]. After the redshift is accounted for it becomes apparent that spectral information is available at slightly different wavelengths for each star. In order to perform an accurate χ^2 test, it is necessary that $template_n$ and $test_n$ correspond to the flux of the two stars at the same wavelength. This effect is corrected by interpolation: fitting a polynomial to the spectrum

such that the flux at any given wavelength can be estimated. In other words, the polynomial is used to obtain flux values for the test star at exactly the same wavelengths for which there are flux data for the template star. After some consideration, the IDL function Interpol was chosen for this task. Examples of subtracting redshift and interpolation can be seen in the Fig. 2.

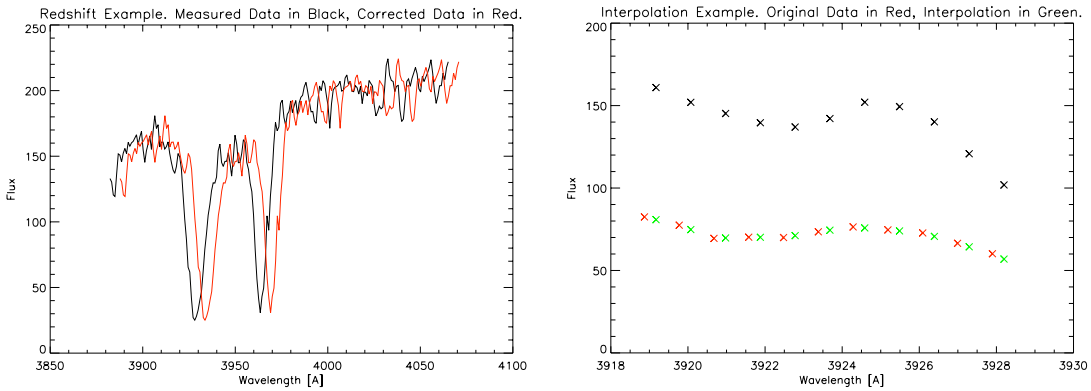

Figure 2: The effect of subtracting redshift from a stellar spectrum (left). On the right, the process of interpolation is shown. The red and black points correspond to the spectra of two stars. Interpolation results in the green points, which are clearly at the same wavelength as the black points. Now, we have spectral information for the two stars at the same wavelengths.

III.3: Flattening and Smoothing

Looking at the χ^2 equation, one can see that a significant difference in the apparent magnitude (or received flux) of two stars being compared will result in a high χ^2 value. One would expect a low signal test star to match poorly when compared against a high signal template, and the fact that very noisy spectra will be difficult to classify cannot be avoided. In order to correctly classify stars, however, it is necessary that χ^2 values reflect how similar spectra are in structure – not simply differences in apparent brightness. Furthermore, as stars can be modeled fairly accurately as blackbodies, the

flux received from a star varies significantly as a function of wavelength resulting in stellar spectra having a distinctive curvature. The shape of the spectrum is heavily dependent on the surface temperature of a star, and even slight differences in the shape of two spectra can also have a dominating effect on the total χ^2 value.

Both of these issues can be resolved by normalizing the spectra such that the flux is consistently close to 1. This "flattening" process removes the previously described curvature as well as eliminates the dominant effect associated with significantly different apparent magnitudes. Similar to interpolation, the flattening process involves fitting a high order polynomial to a spectrum. Next, the flux value at each pixel is divided by the associated value given by the polynomial. Specifically, the IDL function poly_fit was used to fit a 5^{th} order polynomial to the spectra. The process is illustrated in Fig. 3 below.

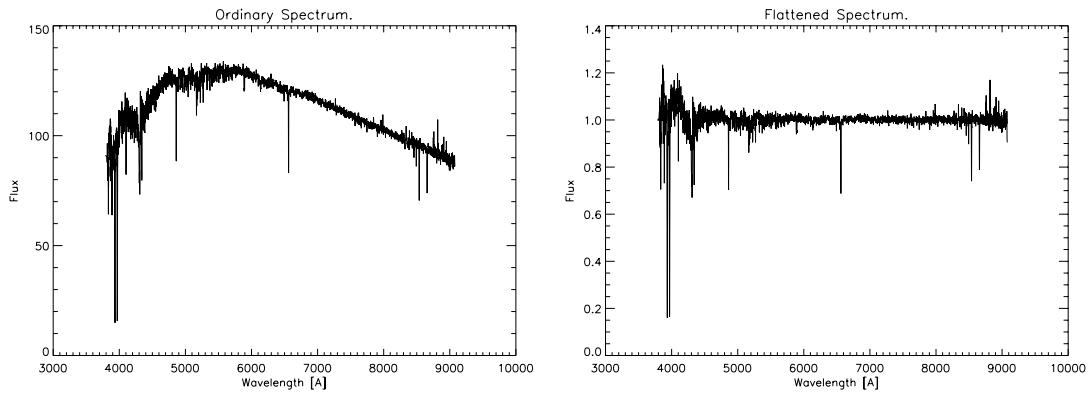

Figure 3: Original spectra (left) with a very strong slope. The same spectra "flattened" is shown on the right. Note the slope is no longer apparent, but the strong structure in the 4000-5000 Å range is preserved.

Another technique, called "smoothing", is invoked in an effort to eliminate small features in the spectra that are unlikely to correspond to significant physical features of the star. Smoothing in this context involves dividing a spectrum by a moving average; the flux value at each pixel is divided by the average value of the flux at nearby pixels within a given range. IDL was used to smooth the spectra, using a moving average of 500 pixels.

A much more dramatic example of smoothing, such that the effects are clearly visible, is shown below in Fig. 4.

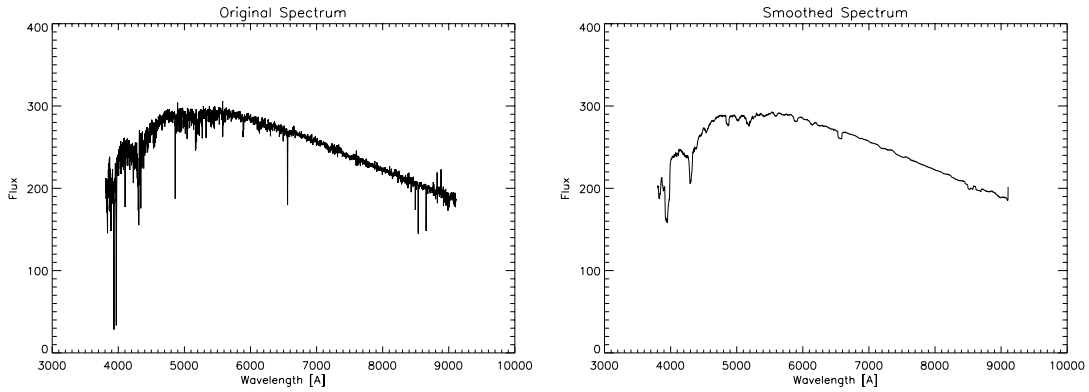

Figure 4: An example of the effects of smoothing, using a 50 pixel moving average. The smoothed spectrum (right) maintains only the overall shape of the original, and not minor details.

The complete flattening procedure therefore consists of initially dividing a spectrum by a fitted 5^{th} order polynomial, thereby flattening it, and then smoothing the resulting spectrum. The final flattened/smoothed spectrum is given by dividing the initially flattened spectrum by this smoothed spectrum. This results in a spectrum where some of the smaller features have been made negligible. Lastly, when flattening test stars, it is necessary to ensure that the estimated noise values correspond to the new scale of the spectrum. Thus, the noise values are manipulated in exactly the same manner. That is, the value of the noise at a given pixel is divided by the same numbers and in the same order as the original value of the flux.

III.4: Comparison Technique

Once two spectra have been flattened, and the necessary interpolation procedure has been completed, the reduced χ^2 test can be performed. A test star is then classified by comparing it in this manner to every giant and dwarf template star that has a color value within 0.025 of its own. The χ^2 values corresponding to the selected templates are then averaged such that there remains an average χ^2 value corresponding to the giant

templates, and another to the dwarfs. Since a strong similarity between two spectra is represented by a small χ^2 value, the classification of a test star as either a giant or dwarf is simply determined by which of the average χ^2 values is smaller. This technique has been refined based on results from a variety of tests, which are the subject of section IV.

IV: DISCUSSION AND ANALYSIS

IV.1: Metallicity Dependence and Modifications to the Template Library.

The classification technique described in section III is the end result of many modifications made based on the results from a number of tests. In particular, the globular cluster M13 proved to be a crucial component in performing these tests. A globular cluster refers to a dense group of stars, typically hundreds of thousands or even millions, which are all approximately the same distance away from the Earth. If the distance to a cluster can be well estimated, the apparent magnitudes of stars in the cluster can be easily converted to absolute magnitudes, and thus the intrinsic luminosity of the stars can be determined. The isochrones plotted in Fig. 1 are an illustration of this technique. Furthermore, it is believed that the stars in a globular cluster originally formed from the same gas, and therefore their atmospheres should be very similar in metallicity. Due to the consistency of these properties, having a library of M13 templates was crucial to the development of the new classification technique.

One of the tests took advantage of the known metallicity of the M13 giants and resulted in a significant reduction of the template library. Each template star was compared against every M13 giant within 0.025 of the template star's color. As described in section III, the template spectra were treated as though they were exact, and thus no errors were involved in computing the χ^2 values for this test (the χ^2 values were not "reduced"). The χ^2 values for the M13 giants within the color range were then averaged, resulting in one average χ^2 per template. These average values were then plotted against metallicity with the expectation that there would be a "dip" at around the metallicity of the M13 giants. This trend would demonstrate that test stars match the templates better if

they are similar in metallicity. It was also expected, since the M13 stars are all known to be giants, that the giants would typically have lower χ^2 values than the dwarfs. Two plots, one for giants and another for dwarfs, are shown below.

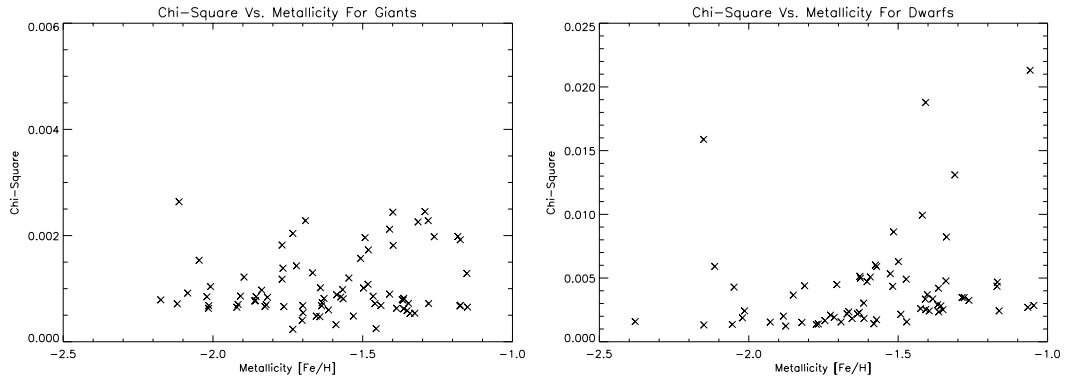

Figure 5: A test aimed to verify the hypothesis that a test star will match better to templates close to itself in metallicity. The expected trend appears not to be significant.

Looking at the scale of the vertical axes of these plots, it is clear that the giants typically match the M13 stars better than the dwarfs. More importantly, while the matching did seem to improve in some cases near the metallicity of the M13 giants (~-1.6), the trend is not very significant; many templates were still producing χ^2 that are much higher in this region than expected. The next task became figuring out why the expected metallicity trend failed to occur. Due to the fact that metallicity is defined in terms of the abundance of Iron, it seemed plausible that significant variations in carbon abundance could help explain the absence of the expected metallicity trend. It was therefore thought that the spectral lines associated with the molecular carbon G-Band might have had a significant effect on the overall χ^2 values. To test this idea, the G-band was excluded from the comparison region[8]. Unfortunately, while the average χ^2 values did change slightly, the plots themselves looked almost identical; there were no

[8] Specifically, the wavelength range of 4250-4450 Å was excluded from the comparison region.

significant changes in the placement of the points and the expected trend in metallicity remained absent. Nevertheless, this result remained very useful as it suggested that there is no need for the classification procedure to account for variations in the abundance of carbon.

It was then considered that another possible explanation for the high χ^2 values could be that the template stars were not actually being compared with M13 stars that were similar to them in color. Due to the fact that stars in a globular cluster are close together in the sky, it is difficult to ensure that all of the photons detected when observing a star in a cluster originated from it. This makes errors in photometric measurements much more likely to occur, which leads to the assumption that the colors of the M13 giants were in fact incorrect. Fortunately, a recent publication includes new photometric data for stars in multiple clusters that were observed as part of SDSS, including M13 [An et al., 2008]. Simply matching the Right Ascension (RA) and Declination (DEC) of the M13 templates gave updated photometric data for eight of the stars. Unfortunately, the methods used by An et al. provided limitations on the apparent magnitudes.

The RA/DEC matching gave new apparent magnitudes through the green filter, but not the red, for an additional six M13 stars. By taking advantage of the isochrones plotted in Fig. 1, new color values could be interpolated (however, the isochrones need to be plotted in terms of the absolute magnitude through the green filter). Since stars in a globular cluster are all approximately the same distance away the same "distance modulus", defined as the difference in apparent and absolute magnitude, can be used for any star. Thus, by estimating the absolute "green" magnitudes of the six M13 stars, and using the giant branches of the two isochrones shown in Fig. 1, new color values were

calculated using the IDL function Interpol. The M3 isochrone proved particularly useful because the data composing the giant branch extends to significantly higher colors than the giant branch of the M13 isochrone. The distance modulus used depends on which cluster was needed for the interpolation process.

Unfortunately, new color values could not be obtained for another six of the stars. The color range spanned by the M13 giants, using the new photometric data, was approximately 0.5-0.8. Due to the fact that there are many thousands of stars in the SDSS database within this range, and because of the importance of the results of other tests based upon the M13 giants (see section IV.2), the decision was made to focus on classifying test stars within this color range. The template library was then reduced accordingly. The previously described test was repeated with the new M13 colors and the restricted color range, resulting in Fig. 6.

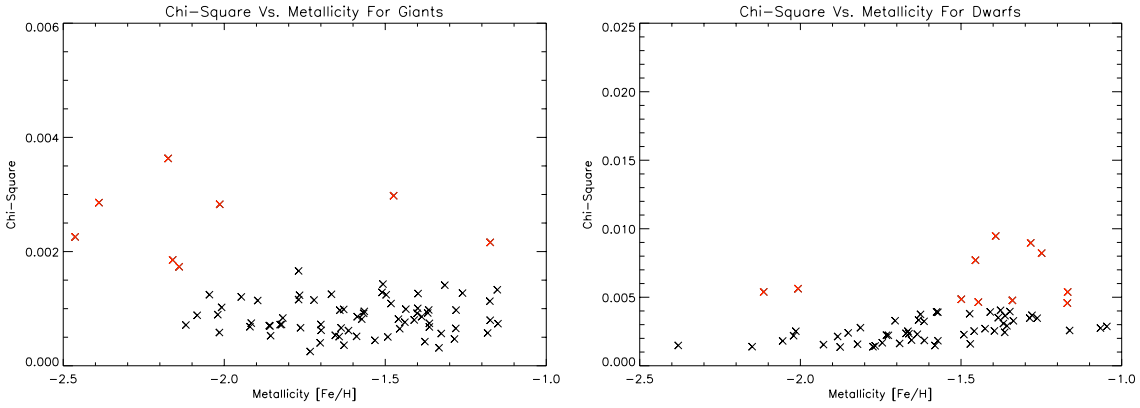

Figure 6: The test resulting in Fig 5 is repeated with new M13 colors and restricted template library. Red points represent "high matching" template stars which will be removed from the library.

While the plots clearly demonstrated that using the updated colors for the M13 giants had a significant impact on many of the χ^2 values, the expected trend in metallicity remained absent. This result seemed to imply that there was no need to ensure that a test star had approximately the same metallicity as the template stars it was being compared against (at least when the test star's metallicity was well within the range spanned by the

template library). The plots also show that a small portion of the template stars, marked by the red points, matched the M13 stars very poorly compared to the other template stars. There are many possible reasons for the bad matches, including significant errors in color and metallicity, or some other problem with the spectra such as missing sections. In any case, the poorly matching stars were removed from the template library.

A few more modifications to the list of template stars were necessary. The test described above leading to Fig. 5/6 did not include some of the template stars, which is why there are significantly less than 224 combined points on the plots. Some template stars simply did not have any M13 giants within 0.025 of its color, thus they could not be compared with anything. In addition, the test program checked to make sure that the χ^2 values for every M13 giant within the color range did not differ significantly. That is, if the largest M13 χ^2 value differed from the smallest by more than 0.0005, the template was left out of the test because there was concern that such inconsistencies would skew the χ^2 averages and produce unfair points on the plots.

The next task was to determine whether or not these templates actually needed to be removed from the library. To test this, the stars were returned to the template library and every star were tested against the M13 giant closest in color – even if the difference in color was greater than 0.025. If the χ^2 value of a removed star was similar to those of the template stars surviving the previous tests, the star was returned to the library. That is, if the removed star matched well with the closest M13 giant, even with a color difference greater than 0.025, the assumption was made that it would be fair to compare that star against any test stars that actually are within 0.025 of its color. Thus, such stars were returned to the template library.

IV.2: Noise Added M13 Spectra as Test Data

It was clear at this point that the classification technique seemed to be working: giants were matching better against the M13 giants than the dwarfs were. However, the previous tests only involved strong signal template stars and thus offered no information as to whether or not this method works with noisy test spectra. Obviously, confidence of the classification of stars needed to be quantified as a function of S/N. Tests aimed at exactly this involved adding noise to the real spectra of the M13 giants. Thousands of noisy versions of the M13 spectra were created by adding real noise from other observations, taken as a part of SDSS/SEGUE, to the M13 spectra [Yanny et al., 2009]. These noisy realizations of the spectra were created for 17 of the original 20 M13 giants, 11 of which have colors between 0.5 and 0.8, with signal to noise (S/N) ratios varying from approximately 1-56.

A test was performed that is very similar to the actual classification technique. As there was now considerable noise associated with the test spectra, the χ^2 tests are reduced as described in section III. For each M13 giant, every giant and dwarf template within 0.025 of the M13 star's color was selected. The noisy realizations were grouped by S/N ratio into bins of 5: approximately 1-6, 6-11, etc. Every noisy spectrum within each S/N bin was compared against every selected template. The χ^2 values were then averaged such that there was, for every noisy spectrum, one χ^2 value corresponding to the giants and another to the dwarfs. The classification of each noisy spectrum was simply determined by which of these averages was larger. The percentage of correct classifications within each S/N bin for every M13 giant (for which noisy spectra were created) was outputted to a table, an example of which is shown below.

M13 Giant Fiberid, Color: 143,0.56												
Value	1.0-6.0	6.0-11.0	11.0-16.0	16.0-21.0	21.0-26.0	26.0-31.0	31.0-36.0	36.0-41.0	41.0-46.0	46.0-51.0	51.0-56.0	> 56.0
Giants %	60.078	70.543	83.247	91.237	91.237	89.005	92.632	93.443	94.211	96.316	95.429	89.474
Dwarfs %	39.922	29.457	16.753	8.763	8.763	10.995	7.368	6.557	5.789	3.684	4.571	10.526

Table 1: An example of classification results for noisy versions of M13 spectra.

These results were quite encouraging. The ability to correctly classify 83% of test stars with a S/N ratio between 11 and 16 could certainly lead to the development of a large library of distant halo stars. Nevertheless, there remained a couple of concerns about the fairness of the averaging techniques used in this test. The fact that the code averages the χ^2 values associated with every giant or dwarf template within the color range could easily hide the fact that some of the templates were matching very poorly and skewing the averages. If true, the removal of these troublesome template stars could result in higher percentages of correct classifications.

To investigate whether or not this was occurring, every noisy spectrum was compared to every giant/dwarf template within 0.025 of the M13 star's color, as before. This time, however, the χ^2 values associated with every noisy spectrum (within each S/N bin for each M13 star) were averaged such that there remained one χ^2 value for every selected giant and another for every selected dwarf. Next, treating giants and dwarfs separately, these average χ^2 values were themselves averaged. This new value was then subtracted from the χ^2 values associated with each selected template, such that there now remained one "delta- χ^2" value for every selected template. The delta- χ^2 values resulting from this somewhat complicated arithmetic are a measure of how well the selected giant or dwarf templates agree with one another about the classification of the relevant noisy spectra. A delta- χ^2 value significantly higher than those of the other selected templates means the template consistently results in unreasonably high χ^2 values and thus, as with previously discussed high matching templates, should be removed from the library. An example of the plots created in search of these templates is shown in Fig 7.

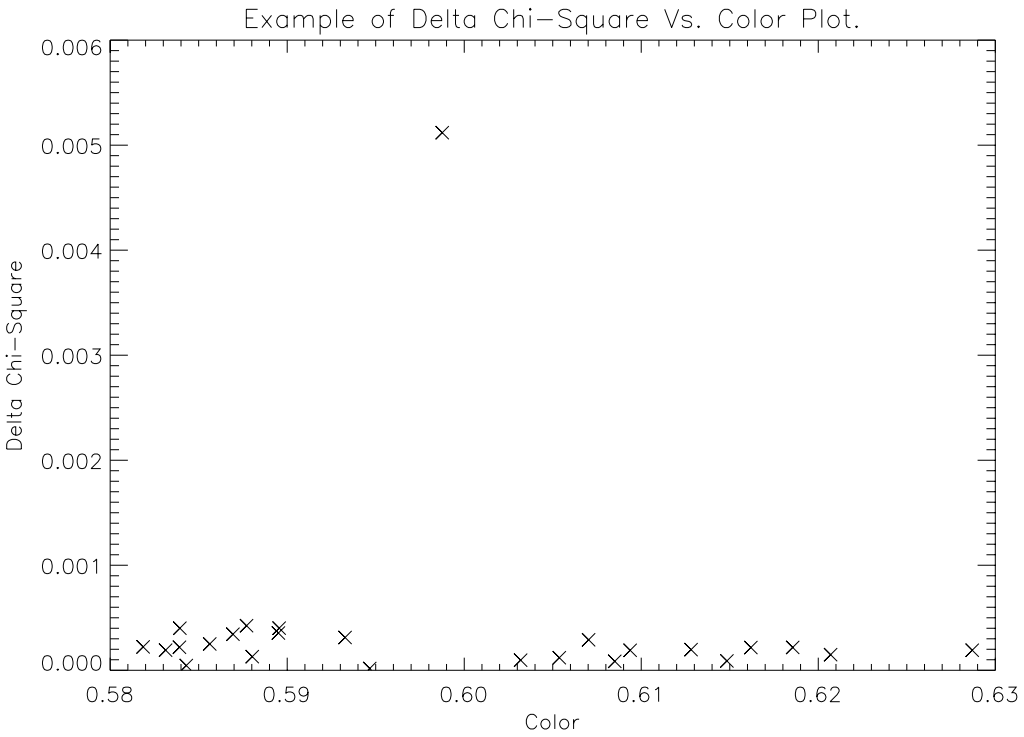

Figure 7: An example of a plot of delta χ2 vs. template star color. Clearly, the delta χ2 value associated with one template is much larger than the others. This star was removed from the library.

This process resulted in the removal of 11 additional stars from the template library. There are no intentions of making additional modifications to the template library, which currently consists of 155 stars as described in section II. However, before classification of actual test stars could begin, another aspect of the noisy M13 test had to be investigated. For the test results to be meaningful, noisy spectra that have approximately the same S/N values should produce similar χ^2 values when compared against the same template stars. Unfortunately, the averaging mechanism used offers no guarantee of this. To investigate, histograms were created of the χ^2 values associated with every noisy spectrum within each S/N bin. That is, for a given M13 giant and a given S/N bin, every selected giant and dwarf template was compared against every noisy spectrum. Treating giants and dwarfs separately, histograms of the χ^2 values were created. An example is shown in Fig 8.

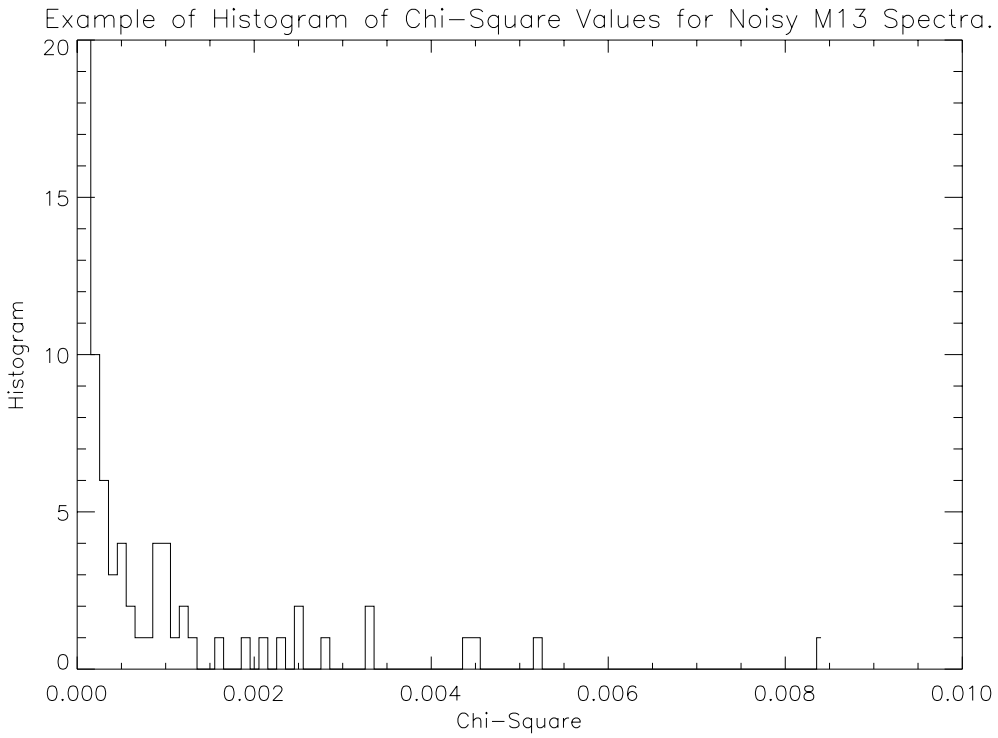

Figure 8: A zoomed in example of a histogram of noisy M13 spectra. Clearly there are outlier spectra, which skew the average of the $\chi 2$ values, which need to be investigated.

As shown above, there were indeed outlier spectra that had been skewing the averages of the χ^2 values. Upon investigation, it became apparent that these spectra have unrealistic spikes associated with an emission line at 5575 Å. Due to the fact that this spike had not previously been present in the M13 giant spectra, it is clear that this particular emission line, corresponding to molecular oxygen, was introduced by adding the noise. However, while the added noise is in a sense fake, it was actually obtained from other SDSS/SEGUE observations [Yanny, et al., 2009]. To make sure this problem does not effect the classification of actual test stars, the line at 5575 Å was removed from the comparison region. An example of this troublesome emission line is shown in Fig. 9.

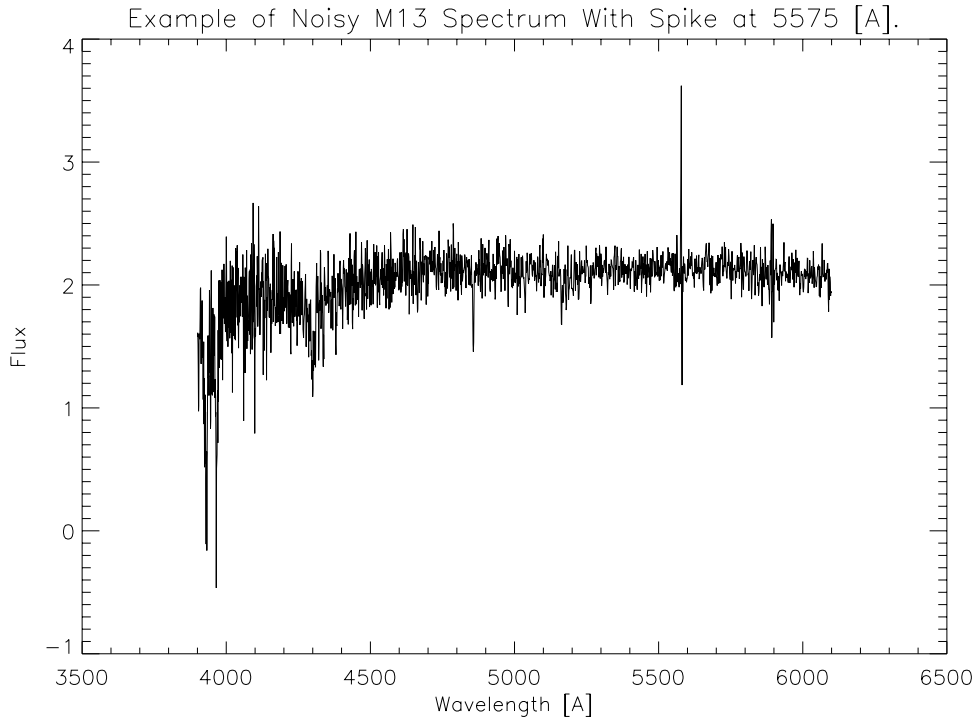

Figure 9: An example of one of the outlier spectra, clearly showing the troublesome O_2 emission line at 5575 Å.

With the problematic template stars removed and the oxygen emission line left out of the comparison region, the noisy M13 spectra were once again compared against the template stars in the same manner as previously described. Once again, the percentage of correct classifications was outputted to a table; an example of which is shown below.

M13 Giant Fiberid, Color: 143,0.56												
Value	1.0-6.0	6.0-11.0	11.0-16.0	16.0-21.0	21.0-26.0	26.0-31.0	31.0-36.0	36.0-41.0	41.0-46.0	46.0-51.0	51.0-56.0	> 56.0
Giants %	62.016	79.07	93.557	96.392	99.485	99.476	100	99.454	100	100	99.429	100
Dwarfs %	37.984	20.93	6.443	3.608	0.515	0.524	1.579	0.546	1.579	1.579	0.571	15.789

Table 2: An example of the classification results for the noisy versions of M13 spectra after final template adjustments have been made. Furthermore, the skyline at 5575 Å was avoided.

As expected, the percentages have somewhat improved. It seems, after an analysis of all of the classification results, that test stars with S/N ratios of 11.5 or greater can be classified correctly at least 90% of the time. These results are very encouraging and suggest that a large library of distant halo giants is well within reach. The testing and

development of the classification technique is complete. Using the process outlined in section II, it is now time to attempt to classify real faint test stars.

V: RESULTS AND CONCLUSIONS

The task of developing a library of distant halo giants is nearly complete. Every star in the online SDSS DR7 database with a S/N ratio of at least 11.5, color between 0.50 and 0.75, and metallicity between -2.5 and -1.0 was retrieved. Of these 18,924 stars, 9668 have been initially classified as giants! A library of almost 10,000 giants would certainly provide an adequate number of test particles for the task of mapping the gravitational potential of the galaxy. Unfortunately, while the end is in sight, there remains much work to be done. For example, there are nearly 60,000 additional stars in the DR7 database that, while they are within the required ranges of color and S/N ratio, are outside the metallicity range spanned by the template stars. Additional tests and analysis will be required to determine whether or not these stars can be classified with reasonable confidence using the stars currently in our template library.

As for the nearly 10,000 stars that have been potentially classified as giants, the next step in the process will be to estimate distances to these stars. This will be done by once again taking advantage of isochrones such as those plotted in Fig 1. The fundamental principle is that the globular cluster isochrones allow one to calculate the absolute magnitude of a star based on its color, so long as it is known whether the star is a giant or a dwarf. The giant branch of the M13 or M3 isochrones shown in Fig 1 could be used to interpolate the correct absolute magnitudes of the test stars, which can then be converted to distance using (2). This, however, must be done carefully as the metallicity of the cluster affects the brightness of the stars and therefore the shape of the isochrones. Fig 1 demonstrates this effect, as M3 and M13 differ slightly in metallicity [An et al.,

2008]. Consequently, various isochrones will be used to account for the differences in metallicity of the test stars.

As the ultimate goal of this study is to map the gravitational potential of the galaxy, the distances to these stars from the center of the galaxy must be calculated as well. This process merely requires some trigonometric calculations involving the RA and DEC of the test stars, the distance of the Earth from the galactic center, and the estimated distances to the stars from Earth. Once these distances have been obtained, the stars can then be used as test particles in the galaxy's gravitational well. It is expected that a library of halo stars, including their distances from the center of the galaxy, will be finalized by August 2009.

Acknowledgements

I would like to acknowledge Professor Constance Rockosi for giving me the wonderful opportunity to work extensively on this project, which has allowed me, as an undergraduate student, to experience a glimpse of life as a research scientist. This work would certainly not have been possible without her continuous guidance and assistance. Additionally, I want to thank Jennifer Gordon and Jesse Sherer for spending many hours proof reading and editing this thesis with me. Lastly, I want to think James Mason for the various advice he has given me relating to the formatting and presentation of this paper.

References

1) An, D., et al. 2008, ApJS, 179, 326A

2) Ryden, Barbara Introduction to Cosmology. San Francisco, CA: Addison Wesley, 2003.

3) "SDSS Data Release 7." Sloan Digital Sky Survey, 2009. http://www.sdss.org/dr7/

4) Serway, Raymond A. Physics for Scientists and Engineers. Belmont, CA: David Harris, 2004.

5) Shu, Frank H. The Physical Universe: An Introduction to Astronomy. Mill Valley, CA: University Science Books, 1982.

6) Tipler, Paul A. and Llewellyn, Ralph A. Modern Physics Fourth Edition. New York, NY: W.H. Freeman and Company, 2003.

7) Yanny, B., et al. 2009, AJ, 137, 4377

Appendix

The following table consists of the plate, modified Julian date (mjd), and fiberid of the final list of template stars[9]. This information is listed in place of traditional coordinates due to the fact that stars are identified by these parameters in the SDSS DR7 database. Color and metallicity are also listed in the table because they are the most relevant data to this project. Lastly, the initial classification as either giant or dwarf is listed, with the M13 giants specifically noted.

Plate	MJD	Fiberid	Color	Metallicity	Type
2181	53524	494	0.608	-1.57	Giant
2312	53709	40	0.561	-1.74	Giant
2312	53709	494	0.653	-2.00	Giant
1914	53729	11	0.753	-2.27	Giant
2047	53732	630	0.595	-1.57	Giant
2304	53762	620	0.631	-1.77	Giant
2304	53762	621	0.592	-1.53	Giant
2387	53770	131	0.671	-1.45	Giant
2390	54094	58	0.589	-2.09	Giant
2390	54094	91	0.639	-2.02	Giant
2558	54140	506	0.662	-1.35	Giant
2558	54140	594	0.562	-1.50	Giant
2689	54149	271	0.615	-1.54	Giant
2452	54178	475	0.594	-2.18	Giant
2452	54178	477	0.578	-1.84	Giant
2557	54178	385	0.578	-1.48	Giant
2557	54178	561	0.571	-1.37	Giant
2389	54213	378	0.626	-1.80	Giant
2176	54243	127	0.653	-1.29	Giant
2176	54243	183	0.615	-1.89	Giant
2449	54271	442	0.610	-2.00	Giant
2311	54331	479	0.607	-1.55	Giant
2799	54368	566	0.576	-1.70	Giant
2624	54380	64	0.610	-1.71	Giant
2624	54380	204	0.643	-1.79	Giant
2816	54400	131	0.742	-2.01	Giant
2853	54440	290	0.767	-1.44	Giant
2853	54440	551	0.579	-1.19	Giant
2857	54453	243	0.585	-1.52	Giant
2857	54453	447	0.585	-1.86	Giant

[9] Plate, mjd, and fiberid are entries in the specObjAll table of the DR7 online database.

2849	54454	265	0.631	-1.72	Giant
2850	54461	136	0.753	-2.17	Giant
2850	54461	546	0.558	-1.68	Giant
2856	54463	212	0.664	-1.26	Giant
2856	54463	232	0.656	-1.39	Giant
2856	54463	460	0.615	-1.25	Giant
2862	54471	195	0.624	-1.20	Giant
2862	54471	212	0.577	-1.53	Giant
2854	54480	151	0.639	-1.55	Giant
2915	54497	173	0.583	-1.44	Giant
2915	54497	214	0.644	-1.42	Giant
2915	54497	329	0.563	-1.83	Giant
2915	54497	335	0.629	-1.45	Giant
2447	54498	202	0.636	-1.61	Giant
2447	54498	329	0.629	-2.09	Giant
2858	54498	335	0.647	-1.40	Giant
2939	54515	372	0.694	-1.56	Giant
2893	54523	173	0.564	-1.66	Giant
2893	54523	258	0.583	-1.92	Giant
2893	54523	259	0.665	-1.55	Giant
2913	54526	147	0.675	-1.51	Giant
1894	53240	296	0.535	-1.55	Giant
1898	53260	602	0.524	-1.76	Giant
1902	53271	238	0.505	-1.98	Giant
1910	53321	221	0.533	-1.35	Giant
1910	53321	525	0.540	-1.49	Giant
1910	53321	530	0.557	-1.40	Giant
2054	53431	406	0.569	-1.53	Giant
2181	53524	559	0.551	-1.33	Giant
2183	53536	99	0.723	-1.75	Giant
2251	53557	89	0.656	-1.82	Giant
2251	53557	107	0.624	-1.50	Giant
2251	53557	175	0.587	-2.08	Giant
2249	53566	177	0.568	-1.82	Giant
2250	53566	325	0.760	-1.51	Giant
2252	53613	141	0.524	-1.32	Giant
2310	53710	117	0.549	-1.53	Giant
2384	53763	181	0.505	-1.60	Giant
2045	53350	175	0.741	-2.31	Giant
2055	53729	352	0.633	-1.45	Giant
1906	53293	256	0.806	-2.04	Giant
2384	53763	481	0.784	-1.56	Giant
2047	53732	640	0.780	-2.11	Giant
2255	53565	143	0.560	-1.60	M13 Giant
2255	53565	148	0.572	-1.60	M13 Giant
2255	53565	116	0.557	-1.60	M13 Giant
2255	53565	490	0.535	-1.60	M13 Giant

2255	53565	551	0.634	-1.60	M13 Giant
2255	53565	120	0.606	-1.60	M13 Giant
2255	53565	510	0.597	-1.60	M13 Giant
2255	53565	483	0.638	-1.60	M13 Giant
2255	53565	463	0.711	-1.60	M13 Giant
2255	53565	468	0.755	-1.60	M13 Giant
2255	53565	474	0.702	-1.60	M13 Giant
2255	53565	488	0.723	-1.60	M13 Giant
2255	53565	152	0.698	-1.60	M13 Giant
2255	53565	487	0.808	-1.60	M13 Giant
2940	54508	470	0.546	-1.73	Dwarf
2799	54368	439	0.539	-1.07	Dwarf
2624	54380	198	0.572	-1.81	Dwarf
2858	54498	489	0.564	-1.56	Dwarf
2447	54498	616	0.557	-1.52	Dwarf
2865	54503	562	0.566	-1.77	Dwarf
2857	54453	312	0.583	-1.52	Dwarf
2315	53741	13	0.522	-0.93	Dwarf
2690	54211	489	0.574	-1.39	Dwarf
2047	53732	59	0.587	-1.98	Dwarf
2315	53741	242	0.582	-2.08	Dwarf
2873	54505	633	0.584	-1.26	Dwarf
2386	54064	150	0.586	-1.14	Dwarf
2304	53762	538	0.578	-1.75	Dwarf
2864	54467	57	0.590	-1.22	Dwarf
2381	53762	63	0.584	-1.49	Dwarf
2558	54140	418	0.578	-1.18	Dwarf
2387	53770	140	0.588	-1.65	Dwarf
2387	53770	458	0.595	-1.33	Dwarf
2182	53905	425	0.568	-1.00	Dwarf
2038	53327	467	0.544	-1.59	Dwarf
2056	53463	194	0.569	-1.91	Dwarf
2314	53713	301	0.590	-1.38	Dwarf
2038	53327	420	0.593	-1.40	Dwarf
2852	54468	206	0.605	-1.62	Dwarf
2038	53327	323	0.588	-1.80	Dwarf
2939	54515	136	0.609	-1.85	Dwarf
1914	53729	393	0.609	-1.36	Dwarf
2939	54515	150	0.613	-1.64	Dwarf
2849	54454	576	0.629	-1.60	Dwarf
2944	54523	490	0.616	-1.91	Dwarf
2868	54451	356	0.607	-1.71	Dwarf
2799	54368	626	0.603	-0.96	Dwarf
2452	54178	357	0.621	-1.52	Dwarf
2848	54453	550	0.615	-1.33	Dwarf
2856	54463	373	0.647	-2.25	Dwarf
1904	53682	569	0.640	-1.68	Dwarf

2940	54508	426	0.619	-1.14	Dwarf
2850	54461	515	0.653	-1.49	Dwarf
2689	54149	570	0.666	-1.52	Dwarf
2816	54400	602	0.662	-1.58	Dwarf
2865	54503	606	0.662	-1.81	Dwarf
2054	53431	484	0.666	-1.58	Dwarf
2890	54495	497	0.666	-1.69	Dwarf
2449	54271	399	0.678	-1.69	Dwarf
2558	54140	628	0.680	-1.51	Dwarf
2856	54463	122	0.670	-1.53	Dwarf
1914	53729	21	0.692	-1.48	Dwarf
2689	54149	518	0.696	-2.09	Dwarf
2457	54180	141	0.698	-1.62	Dwarf
2252	53613	382	0.687	-1.76	Dwarf
2311	54331	290	0.713	-1.84	Dwarf
2865	54503	478	0.706	-1.44	Dwarf
2181	53524	639	0.710	-0.97	Dwarf
2394	54518	459	0.727	-1.93	Dwarf
2849	54454	77	0.734	-2.03	Dwarf
2864	54467	575	0.712	-1.44	Dwarf
2816	54400	583	0.746	-2.01	Dwarf
2457	54180	332	0.737	-1.85	Dwarf
1896	53242	298	0.574	-1.48	Dwarf
2312	53709	615	0.540	-1.50	Dwarf
2315	53741	339	0.543	-1.57	Dwarf
2182	53905	384	0.584	-1.50	Dwarf
2304	53762	68	0.510	-1.16	Dwarf
1894	53240	628	0.504	-1.09	Dwarf
2383	53800	632	0.522	-0.27	Dwarf
1898	53260	98	0.697	-1.71	Dwarf
2539	53918	637	0.687	-1.52	Dwarf